PARAMETRIC STUDY ON REINFORCED CONCRETE JACKETED COLUMNS: COMPARISON OF CHANGES IN BEHAVIOR DUE TO CHANGES IN REINFORCEMENT PATTERN

A. A. Saeem*, M. S. Ahmed, M. M. Rahman, I. Chowdhury & M. R. Alam

Department of Civil Engineering, Chittagong University of Engineering and Technology, Chittagong, Bangladesh
**Corresponding Author: a.al.saeem@gmail.com*

ABSTRACT
This paper contains a parametric study on re-strengthening of rectangular RC columns using different widely practiced RC jacketing techniques. Finite element program ANSYS Multi Physics is utilized for non-linear finite element analysis owing to its capabilities to predict and pictorially represent the response of RC columns in post-elastic range to the ultimate strength. Comparisons are done among four different popular techniques of RC jacketing to find out the link between reinforcement pattern and columns' structural behaviour, i.e., lateral and axial deformation response and crack formation. A rectangular RC column without retrofitting is analysed and then it is retrofitted to a target ultimate strength theoretically in four distinct ways: retrofitted with (i) one reinforcing bar at each corner; (ii) two reinforcing bars at each corner; (iii) three reinforcing bars at each corner with diagonal confinement bar at corners; and (iv) four reinforcing bars at each corner having two layers of additional tie bars and analysed. The study finds the jacketing technique (iii) to be the most efficient for jacket of RC column.

Keywords: ANSYS; finite element analysis; interface; RC column jacketing; re-strengthening

INTRODUCTION
Reinforced concrete members are often damaged due to natural disasters, notably earthquakes, overloading, change in building usage and so on. Damage may take place in almost all parts of a structure, namely slabs, beams, columns, walls etc. Rehabilitation is needed after the damage has taken place to bring the damaged member to the strength previously existed. Re-strengthening is also carried out when the purpose of an existing structure changes, predicted load increases or environmental load increases than that was taken into account when designed. Re-strengthening of reinforced concrete members has become very common in the modern world. There are different retrofitting techniques for different members of a structure. Jacketing is the most popularly used method for strengthening of building columns. The most common types of jackets are steel jacket, reinforced concrete jacket, fiber reinforced polymer composite jacket, jacket with high tension materials like carbon fiber, glass fiber etc. Enlargement of the existing structural members such as column and beam sections by placing reinforcing steel rebars around its periphery and then concreting it is widely adopted option; which is referred as concrete jacketing. This method significantly increases the member sizes and thereby its stiffness. Concrete Jacketing primarily enhances the confinement along with the shear and axial behaviour in case of columns.

There is a wide spectrum of published work on column jacketing. The published work emphasizes finding out the minimum requirements, interface treatment and the failure type. Several experimental and numerical analyses show the minimum requirements for reinforced concrete column jacketing (Vedprakash et. al., 2014, Pravin et. al., 2011). Strength of the new materials will be equal or greater than those of the existing column. Minimum jacket thickness will be 4". All published work on RC jacketing recognize the importance of interface preparation to achieve a good bond between the original column and the added jacket so that the resulting element behaves monolithically (Ju´lio et. al., 2003). The current practice of surface treatment in several countries consists increasing surface roughness, application of bonding agent and application of steel connectors. Hand chipping, sand-blasting, jack-hammering, electric hammering, water demolition and iron brushing are the most common surface

roughening methods. Several authors state that increasing the roughness of the interface surface is necessary, but its influence has not been quantified (Rodriguez et. al., 1994, Bett et. al., 1988, Alcocer et. al., 1990). Several publications conclude that adding steel connectors crossing the interface does not meaningfully increase the debonding force, but increases almost directly the longitudinal shear strength considering slipping (Ju´lio et. al., 2001). In this work, a comparison among various techniques (Teran et. al., 1992) of RC jacketing is done using ANSYS Multi Physics computer program. This study aims to investigate and compute the lateral and axial deformation responses at different stages of axial incremental loading and find the effect of reinforcement pattern on lateral and axial deformation responses and crack formation.

NUMERICAL MODELING IN ANSYS

The concrete material model predicts the failure of brittle materials. An eight-node solid element SOLID65 is used to model the concrete. The solid is capable of cracking in tension and crushing in compression. The element is defined by eight nodes having three degrees of freedom at each node: translations in the nodal x, y and z directions. Link8 element is used to model the steel reinforcement. LINK8 is a 3-D spar element which is a uniaxial tension-compression element with three degrees of freedom at each node: translations in the nodal x, y, and z directions. Interface surface is created using TARGE170 and CONTA174 geometries. For 3D modeling, the surface of old concrete is taken as contact surface and the surface of new concrete is taken as target surface by default. Then a contact pair is created using standard contact behavior. Default values of normal penalty stiffness and penetration tolerance are allowed for the surface to surface contact creation. Maximum friction stress is taken to be $1x10^{20}$ psi.

The criterion for failure of concrete due to a multi-axial stress is controlled by the expression given by Willam and Warnke (1975).

$$F/f_c - S \geq 0$$

where, F = a function of the principal stress state (σ_{xp}, σ_{yp}, σ_{zp}); S = failure surface expressed in terms of principal stresses and five input parameters f_t, f_c, f_{cb}, f_1 and f_2; f_c = uniaxial crushing strength; σ_{xp}, σ_{yp}, σ_{zp} = principal stresses in principal directions. However, the failure surface can be specified with a minimum of two constants, f_t and f_c. The other three constants default to Willam and Warnke:

$$f_1 = 1.45 f_c \; ; \; f_2 = 1.725 f_c \; ; \; f_{cb} = 1.2 f_c$$

These default values are valid only for stress states where the condition

$$|\sigma_h| \leq \sqrt{3}\, f_c \; ; \; \sigma_h = \text{Hydrostatic stress rate} = (1/3)(\sigma_{xp} + \sigma_{yp} + \sigma_{zp})$$

is satisfied. This condition equation applies to stress situations with a low hydrostatic stress component. All five failure parameters should be specified when a large hydrostatic stress component is expected. If condition equation is not satisfied, the strength of the concrete material may be incorrectly evaluated. When the crushing capability is suppressed with f_c = -1.0, the material cracks whenever a principal stress component exceeds f_t.

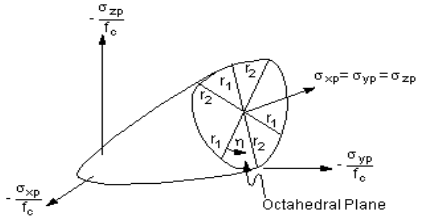

Fig. 1: 3-D failure surface in principal stress space (ANSYS, 2011)

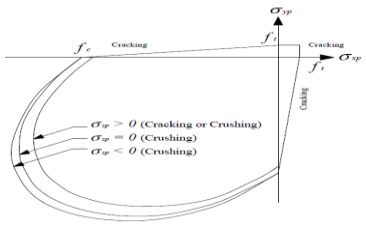

Fig. 2: Failure surface in principal stress space with nearly biaxial stress (ANSYS, 2011)

Both the function F and the failure surface S are expressed in terms of principal stresses denoted as, σ_1, σ_2, and σ_3 where:

$$\sigma_1 = \max(\sigma_{xp}, \sigma_{yp}, \sigma_{zp}); \; \sigma_3 = \min(\sigma_{xp}, \sigma_{yp}, \sigma_{zp}) \text{ and } \sigma_1 \geq \sigma_2 \geq \sigma_3.$$

The failure of concrete is categorized into four domains:

$$0 \geq \sigma_1 \geq \sigma_2 \geq \sigma_3 \text{ (compression - compression - compression)}$$

$$\sigma_1 \geq 0 \geq \sigma_2 \geq \sigma_3 \text{ (tensile - compression - compression)}$$

$$\sigma_1 \geq \sigma_2 \geq 0 \geq \sigma_3 \text{ (tensile - tensile - compression)}$$
$$\sigma_1 \geq \sigma_2 \geq \sigma_3 \geq 0 \text{ (tensile - tensile - tensile)}$$

In each domain, independent functions describe F and the failure surface S. The four functions describing the general function F are denoted as $F1$, $F2$,$F3$, and $F4$ while the functions describing S are denoted as, $S1$, $S2$, $S3$, and $S4$. The functions (i = 1-4) have the properties that the surface they describe is continuous while the surface gradients are not continuous when any one of the principal stresses changes sign. In this work, a 12"x12" column is taken to be re-strengthened. The dimensions of jacket (4" at each side) for all four techniques are kept unaltered. Length of each model is 10 ft. The design is done in such a way that the compressive strength of the four models after re-strengthening are theoretically equal. The design compressive strength for non-jacketed (A) and jacketed (B, C, D, E) columns are 433.8 kips and 1115.2 kips whereas the nominal compressive strength are 667.4 kips and 1715.6 kips respectively. The modelling of interface surface is done in the same way for four models. These conditions ensure that the change in structural responses with incremental loading obtained in numerical analysis will be controlled only by reinforcement pattern.

Table 1: Details of numerical modelling in ANSYS

	A	B	C	D	E
Plan view	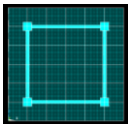	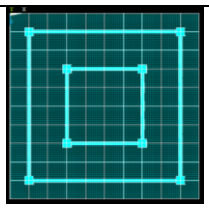	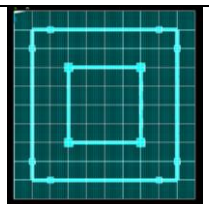	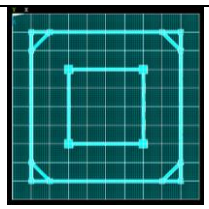	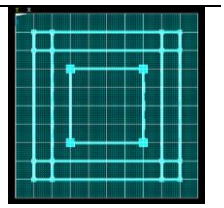
Isometric view	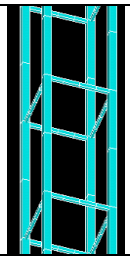	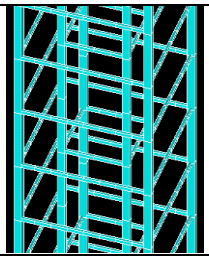	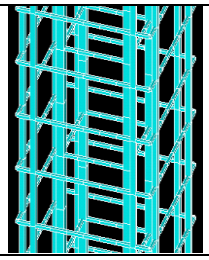	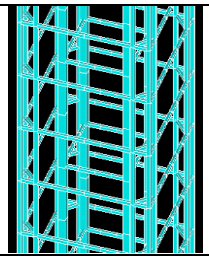	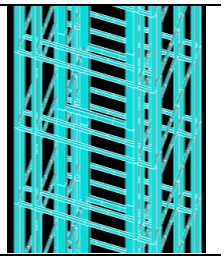
Size	12″x12″	20″x20″	20″x20″	20″x20″	20″x20″
Longitudinal Steel	4#8φ	8#8φ	Equivalent to 8#8φ	Equivalent to 8#8φ	Equivalent to 8#8φ
Transverse Steel	#3φ @12″ c/c	#3φ @6″ c/c	Equivalent to #3φ @6″ c/c	Equivalent to #3φ @6″ c/c	Equivalent to #3φ @6″ c/c

Material Properties

The properties of concrete and reinforcing steel are as the table below.

Table 2: Material Properties

Concrete		Reinforcing Steel	
Property	**Value**	**Property**	**Value**
Compressive Strength	4000 psi	Modulus of Elasticity	2.9×10^7 psi
Modulus of Elasticity	3.605×10^6 psi	Poisson's Ratio	0.3
Poisson's Ratio	0.18	Yield Strength	60000 psi
Uniaxial Cracking Stress	474.34 psi	Tangent Modulus	2900 psi
Open shear transfer coefficient	0.3		
Closed shear transfer coefficient	1		

Element Meshing

After modeling and inputting all the data the models are meshed. The original column (A) is subdivided into 6x6x20=720 elements whereas the retrofitted columns (B, C, D and E) are subdivided into 10x10x20=2000 elements. Each element sizes 2″x2″x6″. The mesh size is kept the same in contact surface i.e. 2″x6″. Number of elements in contact surface is 6x20x4=480.

Loads and boundary condition

Displacement boundary conditions are needed to be constrained in the model to get a unique solution. To ensure that the model acts the same way as the experimental columns specimens, boundary conditions need to be applied where the supports and loadings exist. For concentric columns model the displacement of all nodes at bottom base of column in x, y and z. directions is held zero (Ux=0 , Uz=0 and Uy=0). To apply the axial load on the top of the concentric column specimens, loads were applied on each nodes at the top of the columns.

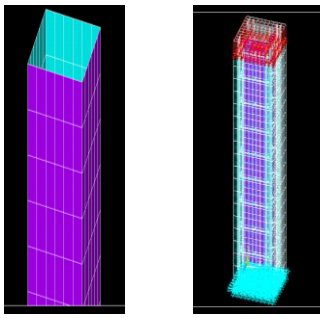

Interface Surface Modelling

Boundary Conditions

Fig. 3: Interface and Boundary Conditions

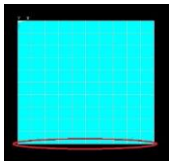

(a) Top view

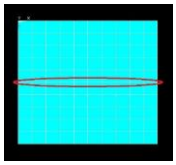

(b) Top view

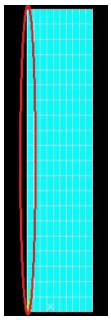

(c) Front view

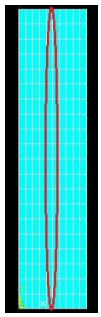

(d) Front view

Fig. 4: Selected directions for structural response comparison

RESULTS AND DISCUSSIONS

In the following section, the four models of RC jacketing will be compared on the basis of load-deflection plots at selected locations on the columns, first cracking loads and loads at failure.

First Cracking Load

The analysis of the five column models shows the following first cracking loads. The increment of the first cracking load with compared to model A is also shown in the Table 3.

Table 3: Comparison of first cracking load

Model	**A**	**B**	**C**	**D**	**E**
First Cracking Load (Kips)	230.6	648.6	619.9	652.1	648.3
Increment (compared to A), %	0.00	181.27	168.82	182.78	181.1

Displacements and Stresses

Four directions are selected for the comparison of displacements and stresses as shown in Fig. 4. Total 72 different comparison are made on displacements (i.e. x-component of displacement, y- component of displacement, z- component of displacement and displacement vector sum) and stresses (i.e. 1st principal stress, 2nd principal stress, 3rd principal stress, stress intensity and equivalent Von Mises stress). Some of the comparisons are shown in Fig. 5 to Fig. 12.

Fig. 5 shows that at top edge nodes of plan displacement is maximum at two opposite sides and decreases from side to middle. Displacement plot shows that displacement both at middle and side are minimum for model D at the same concentric loading condition.

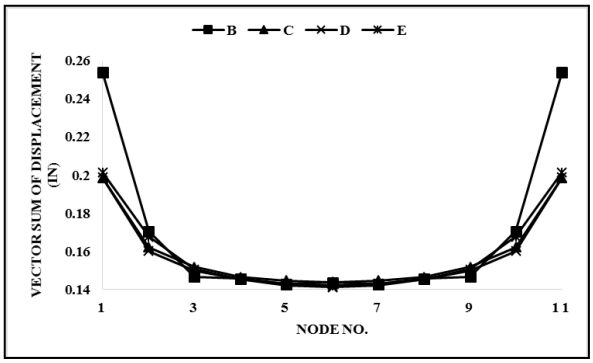

Fig. 5: Variation of Vector Sum of Displacement (direction shown in Fig. 4a)

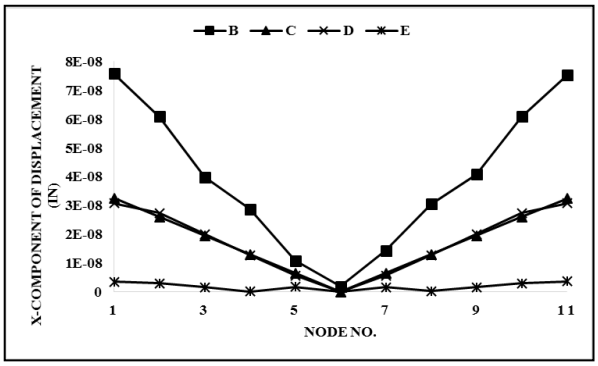

Fig. 6: Variation of x-component of Displacement (direction shown in Fig. 4b)

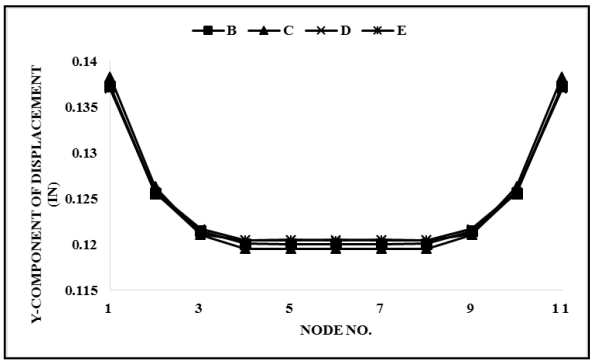

Fig. 7: Variation of y-component of Displacement (direction shown in Fig. 4b)

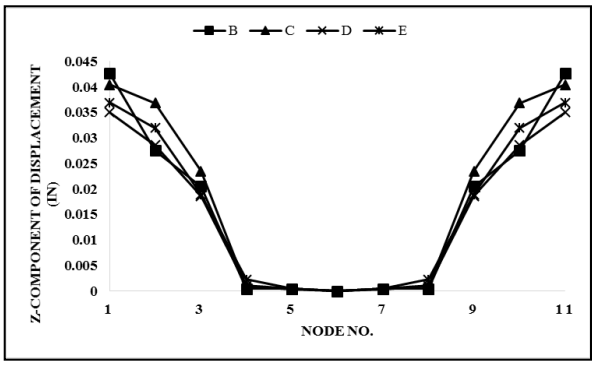

Fig. 8: Variation of z-component of Displacement (direction shown in Fig. 4b)

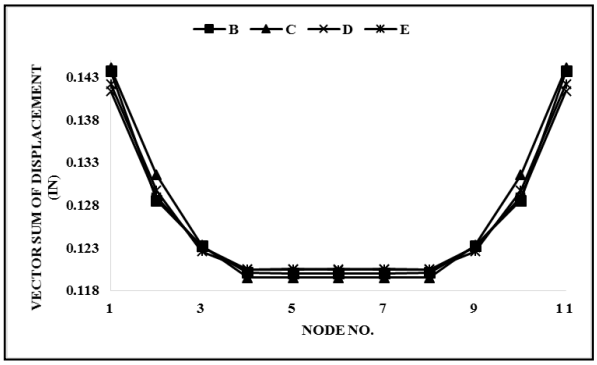

Fig. 9: Variation of Vector Sum of Displacement (direction shown in Fig. 4b)

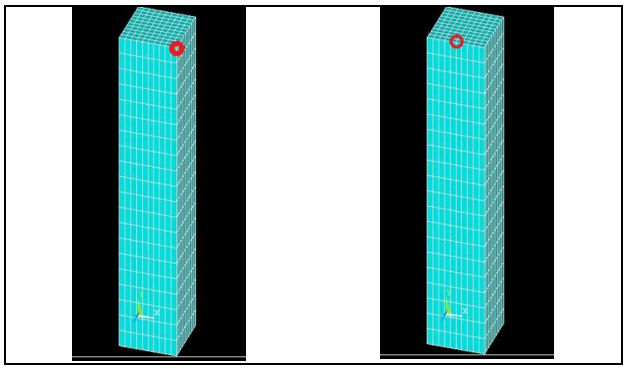

Fig. 10(a): Top corner node location Fig. 10(b): Top edge

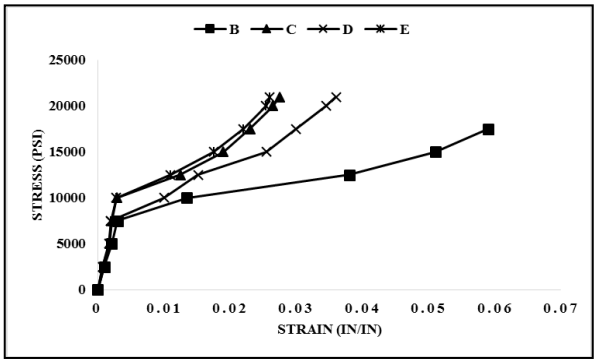

Fig. 11: Stress-strain diagram for top corner node.

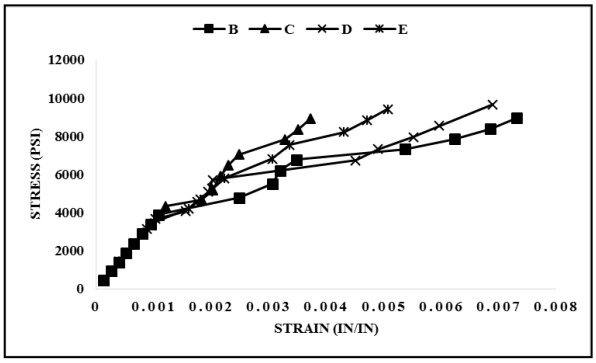

Fig. 12: Stress-strain diagram for top edge middle node

In Fig. 6, it is found that the x-component of displacement is always minimum for model E, then model C, and maximum value for model B. Fig. 7 describes the variation of y-component of displacement at

top middle nodes of plan and shows maximum displacement is for model C at edge whereas minimum displacement is for D at the edge node. The minimum displacement at the center node is for model C. In Fig. 8, the z-component of displacement is minimum for model D and maximum for model B. Displacement value decreases from edge to middle nodes. Fig. 9 describes the variation of vector sum of displacement at top middle nodes of plan and shows minimum displacement is for model D at the edge node whereas maximum displacement is for C. The minimum displacement at the center node is for model C.

CONCLUSIONS

Based on the analysis and comparison of the four different models, conclusion may be stated as: In very low range of loading, the axial and lateral deformation responses of model B, C, D and E are almost similar. From the stress-strain diagram shown in Fig. 11 it can be concluded that all the four models act almost the same upto the proportional limit. After exceeding the proportional limit, the model E shows most brittle behavior. The model C also shows brittle nature whereas the model D shows a relatively flat stress-strain diagram which indicates its ductile nature. The model B also shows maximum strain at the same stress level but the curve ends before reaching the maximum stress level reached by the model D. From the stress-strain diagram shown in Fig. 12, it is established that all the four models act almost the same upto the proportional limit and after exceeding the proportional limit, the model C shows a steeper stress-strain diagram. The model E shows almost same behavior as model C but gives a flatter stress-strain diagram than that of the model C which indicates E to be more brittle than C. The stress-strain diagram for model B is flatter than that of the model D. The model B shows maximum strain at the same stress level as the model D but the curve ends before reaching the maximum stress level reached by the model D. Cracking starts at 652.1 kips load for model D, which is greater than the other three (B=648.6 kips; C=619.9 kips; E=648.3 kips). From the stress-strain diagrams (Fig. 11 and Fig. 12), it is observed that the model D shows more ductile behavior than model C and E. Model D is the best RC jacketing technique based on its axial and lateral deformation responses, such as strain at different stages of incremental loading; stresses at different points; and cracking load.

REFERENCES

A.Teran & J.Ruiz, Reinforced concrete jacketing of existing structures, *Earthquake Engineering, Tenth World Conference*, 1992 Balkema, Rotterdam. ISBN 9054100605.

Alcocer S & Jirsa J. Assessment of the response of reinforced concrete frame connections redesigned by Jacketing. *Proceedings of the 4th US National Conference on Earthquake Engineering* 1990: 3: 295–304.

ANSYS 11.0 user manual, ANSYS Corporation.

Bett BJ, Klingner RE & Jirsa JO. Lateral load response of strengthened and repaired reinforced concrete columns, *ACI Structural Journal* 1988: 85(5): 499–508.

Ju´ lio E S, F Branco and V D Silva, *Structural rehabilitation of columns with reinforced concrete jacketing*, Prog. Struct. Engng Mater. 2003; 5:29–37 (DOI: 10.1002/pse.140).

Ju´ lio ES, Branco F & Dias da Silva V. *A influe^ncia da interface no comportamento de pilares reforc¸ados por encamisamento de beta˜o armado. Proceedings of the Congresso Construc¸a˜o* 2001, IST, Lisbon, 17–19 December 2001: 1: 439–446.

Julio ES., *A influe^ncia da interface no comportamento de pilares reforc¸ados por encamisamento de beta˜o armado*, PhD Thesis, Universidade de Coimbra. 2001.

Rodriguez M & Park R., Seismic load tests on reinforced concrete columns strengthened by jacketing, *ACI Structural Journal*, March–April 1994: 91(2): 150–159.

Shri. Pravin B. Waghmare, Materials And Jacketing Technique For Retrofitting Of Structures, *International Journal of Advanced Engineering Research and Studies* E-ISSN2249 – 8974(2011)

Vedprakash C. Marlapalle, P. J. Salunke, N. G. Gore, Analysis & Design of R.C.C. Jacketing for Buildings, *International Journal of Recent Technology and Engineering (IJRTE)*, ISSN: 2277-3878, Volume-3 Issue-3, July 2014.